International Conference on High Energy Physics
ICHEP2022 – Bologna, July 2022

F Hautmann

Nonperturbative contributions to vector boson transverse momentum spectra: PDF bias and flavor dependence in TMD distributions

based on Phys. Lett. B 806 (2020) 135478 [arXiv:2002.12810], arXiv:2201.07114

thanks to collaborators M. Bury, S. Leal Gomez, I. Scimemi, A. Vladimirov, P. Zurita

DRELL-YAN (DY) PRODUCTION AT qT << Q

- It was realized long ago that DY vector-boson transverse momentum spectra are affected for qT << Q by large dynamical effects beyond collinear factorization:

  - perturbative logarithmically-enhanced corrections in \alpha_s^n \ln^m(Q/qT)

  - nonperturbative contributions besides PDFs due to

    i) intrinsic kT distribution of initial states and

    ii) nonperturbative components of Sudakov form factors.

[Parisi-Petronzio, NPB 154 (1979) 427
Curci-Greco-Srivastava, NPB 159 (1979) 451
Dokshitzer-Diakonov-Troian, Phys Rep 58 (1980) 269
Collins-Soper, NPB 193 (1981) 381]

LOW-qT FACTORIZATION AND EVOLUTION

[Collins-Soper-Sterman, NPB 250 (1985) 199;

Collins, Foundations of perturbative QCD, CUP 2011]

We start from the TMD factorization formula for the differential cross section for DY lepton pair production $h_1 + h_2 \to Z/\gamma^*(\to ll') + X$ at low $q_T \ll Q$ [13]

$$\frac{d\sigma}{dQ^2 dy dq_T^2} = \sigma_0 \sum_{f_1,f_2} H_{f_1 f_2}(Q,\mu) \int \frac{d^2\boldsymbol{b}}{4\pi} e^{i\boldsymbol{b}\cdot\boldsymbol{q}_T} F_{f_1\leftarrow h_1}(x_1,\boldsymbol{b};\mu,\zeta_1) F_{f_2\leftarrow h_2}(x_2,\boldsymbol{b};\mu,\zeta_2) + O(q_T/Q) + O(\Lambda_{\rm QCD}/Q), \quad (1)$$

where Q^2, $\boldsymbol{q}_T$ and y are the invariant mass, transverse momentum and rapidity of the lepton pair, and the TMD distributions $F_{f\leftarrow h}$ fulfill evolution equations in rapidity

$$\frac{\partial \ln F_{f\leftarrow h}}{\partial \ln \zeta} = -\mathcal{D}^f(\mu,\boldsymbol{b}) \quad (2)$$

and in mass

$$\frac{\partial \ln F_{f\leftarrow h}}{\partial \ln \mu} = \gamma_F(\alpha_s(\mu),\zeta/\mu^2) \ , \qquad \frac{\partial \mathcal{D}^f(\mu,\boldsymbol{b})}{\partial \ln \mu} = \frac{1}{2}\Gamma_{\rm cusp}(\alpha_s(\mu)) \ . \quad (3)$$

PHENOMENOLOGICAL STUDIES OF NONPERTURBATIVE TMD EFFECTS

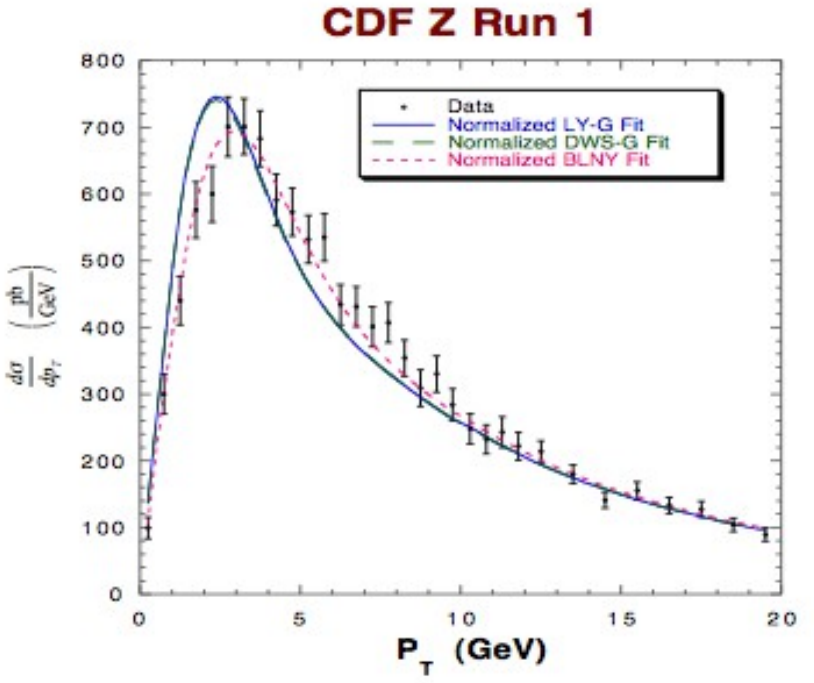

- Pioneering studies by “Resbos”:

[Ladinsky-Yuan, PRD 50 (1994) R4239
Landry et al, PRD 63 (2001) 013004
Landry et al, PRD 67 (2003) 073016
Konychev-Nadolsky, PLB633 (2006) 710]

- Recent “TMD fits”:

Scimemi-Vladimirov, JHEP 06 (2020) 137; Bacchetta et al., JHEP 07 (2020) 117, arXiv:2206.07598

- “Parton branching TMD” determination:

Bermudez Martinez et al., Phys. Rev. D 99 (2019) 074008

EXAMPLE: RECENT DETERMINATIONS OF RAPIDITY EVOLUTION KERNEL *D (b, mu)*

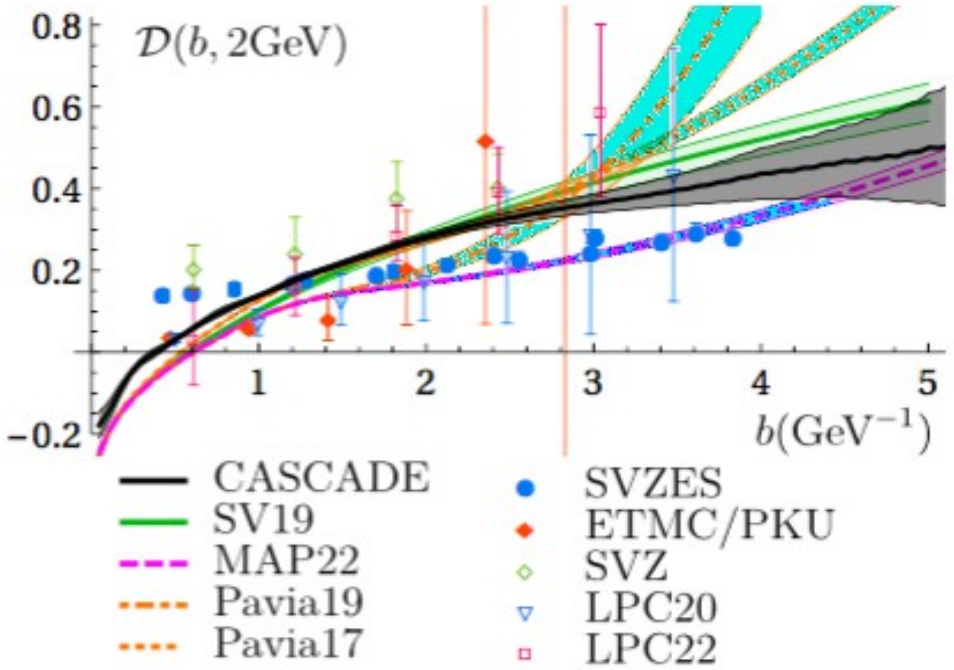

A Bermudez Martinez and A Vladimirov, arXiv:2206.01105

Determinations of kernel *D* from different approaches:
data fits; lattice; TMD Monte Carlo.

- This talk will concentrate on studies (based on arXiv:2002.12810, arXiv:2201.07114) to assess TMD uncertainties in current extractions from fits to experimental data.

A purely factorization-based approach to TMD extraction

Factorization formula of schematic form (up to power corrections):

$$\frac{d\sigma}{dq_T^2} = \sum_{i,j} \int d^2b\, e^{ib\cdot q_T}\, \sigma_{ij}^{(0)}\, f_{1,i\leftarrow h1}(x_1, b; \mu, \zeta_1)\, f_{1,j\leftarrow h2}(x_2, b; \mu, \zeta_2)$$

+ appropriate evolution equations for the TMD distributions *f*

- Measure observable on left hand side; extract *f* on right hand side
- *f* nonperturbative quantity, determined with experimental uncertainties (due to data) and theoretical uncertainties (due to factorization and evolution)

- This would be in the spirit of
  Jung, Mulders, Kraemer, Nocera, Rogers, Signori & H,
  "TMDlib", Eur. J. Phys. C 74 (2014) 3220 [arXiv:1408.3015]

Extraction of TMD distributions using OPE relations

- OPE: *f* is expanded along collinear PDFs, with *b^2* power corrections

$$f_{1,f\leftarrow h}(x,b;\mu,\zeta) = \sum_{f'} \int_x^1 \frac{dy}{y} C_{f\leftarrow f'}(y,b;\mu,\zeta)\, q_{f'}\left(\frac{x}{y},\mu\right) + O(b^2)$$

- Ansatz is made for the large-*b*, nonperturbative *f_NP*

$$f_{1,f\leftarrow h}(x,b;\mu,\zeta) = \sum_{f'} \int_x^1 \frac{dy}{y} C_{f\leftarrow f'}(y,b;\mu,\zeta)\, q_{f'}\left(\frac{x}{y},\mu\right) f^f_{\rm NP}(x,b)$$

and *f_NP* is fitted.

- “PDF bias” (an *f_NP* for every PDF set or PDF replica)

- fits so far include flavor dependence in PDF but not in *f_NP*

INCLUSION OF PDF UNCERTAINTY AND FLAVOR DEPENDENCE IN TMD EXTRACTION

[Bury, Leal Gomez,Scimemi, Vladimirov, Zurita & H, arXiv:2201.07114]

- Represent PDF as MC ensemble
- Uncertainties by fitting each member of input ensemble
- Two uncertainty sources, EXP and PDF

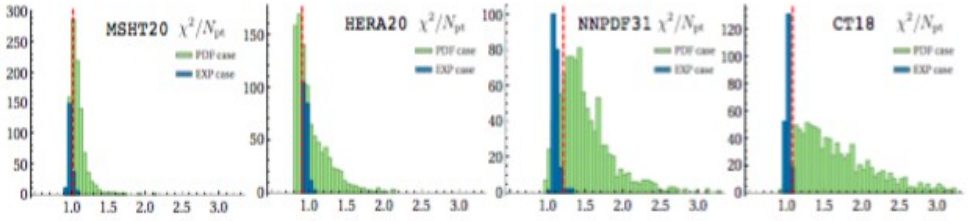

Figure 5: Distribution of χ^2-values for the **PDF** and **EXP** cases. The red lines show the position of the final χ^2-value.

		MSHT20	HERA20	NNPDF31	CT18
Data set	N_{pt}	χ^2/N_{pt}	χ^2/N_{pt}	χ^2/N_{pt}	χ^2/N_{pt}
CDF run1	33	0.78	0.61	0.72	0.75
CDF run2	39	1.70	1.42	1.68	1.79
D0 run1	16	0.71	0.81	0.79	0.79
D0 run2	8	1.95	1.39	1.92	2.00
D0 run2 (μ)	3	0.50	0.59	0.55	0.52
ATLAS 7TeV 0.0<|y|<1.0	5	4.06	1.94	2.12	4.21
ATLAS 7TeV 1.0<|y|<2.0	5	7.78	4.83	4.52	6.12
ATLAS 7TeV 2.0<|y|<2.4	5	2.57	2.18	3.65	2.39
ATLAS 8TeV 0.0<|y|<0.4	5	2.98	3.66	2.12	3.23
ATLAS 8TeV 0.4<|y|<0.8	5	2.00	1.53	4.52	3.21
ATLAS 8TeV 0.8<|y|<1.2	5	1.00	0.50	2.75	1.89
ATLAS 8TeV 1.2<|y|<1.6	5	2.25	1.61	2.49	2.72
ATLAS 8TeV 1.6<|y|<2.0	5	1.92	1.68	2.86	1.96
ATLAS 8TeV 2.0<|y|<2.4	5	1.35	1.14	1.47	1.06
ATLAS 8TeV 46<Q<66GeV	3	0.59	1.86	0.23	0.05
ATLAS 8TeV 116<Q<150GeV	7	0.61	1.03	0.85	0.70
CMS 7TeV	8	1.22	1.19	1.30	1.25
CMS 8TeV	8	0.78	0.77	0.75	0.78
CMS 13TeV 0.0<|y|<0.4	8	3.52	1.93	2.13	3.73
CMS 13TeV 0.4<|y|<0.8	8	1.06	0.53	0.71	1.65
CMS 13TeV 0.8<|y|<1.2	10	0.48	0.14	0.33	0.88
CMS 13TeV 1.2<|y|<1.6	11	0.62	0.33	0.47	0.86
CMS 13TeV 1.6<|y|<2.4	13	0.46	0.32	0.39	0.57
LHCb 7TeV	8	1.79	1.00	1.62	1.16
LHCb 8TeV	7	1.38	1.29	1.63	0.83
LHCb 13TeV	9	1.28	0.84	1.07	0.93
PHE200	3	0.29	0.42	0.38	0.29
E228-200	43	0.43	0.36	0.57	0.43
E228-300 $Q < 9$GeV	43	0.77	0.56	0.89	0.55
E228-300 $Q > 11$GeV	10	0.29	0.37	0.45	0.44
E228-400 $Q < 9$GeV	34	2.19	1.15	1.49	1.34
E228-400 $Q > 11$GeV	42	0.25	0.61	0.44	0.40
E772	35	1.14	1.37	1.79	1.11
E605 $Q < 9$GeV	21	0.52	0.47	0.47	0.61
E605 $Q > 11$GeV	32	0.47	0.73	1.34	0.52
Total	**507**	**1.12**	**0.91**	**1.21**	**1.08**

Table 3: Distribution of the values of χ^2 over the TMD data set in fits with different PDF input.

INCLUSION OF PDF UNCERTAINTY AND FLAVOR DEPENDENCE IN TMD EXTRACTION

[Bury, Leal Gomez,Scimemi, Vladimirov, Zurita & H, arXiv:2201.07114]

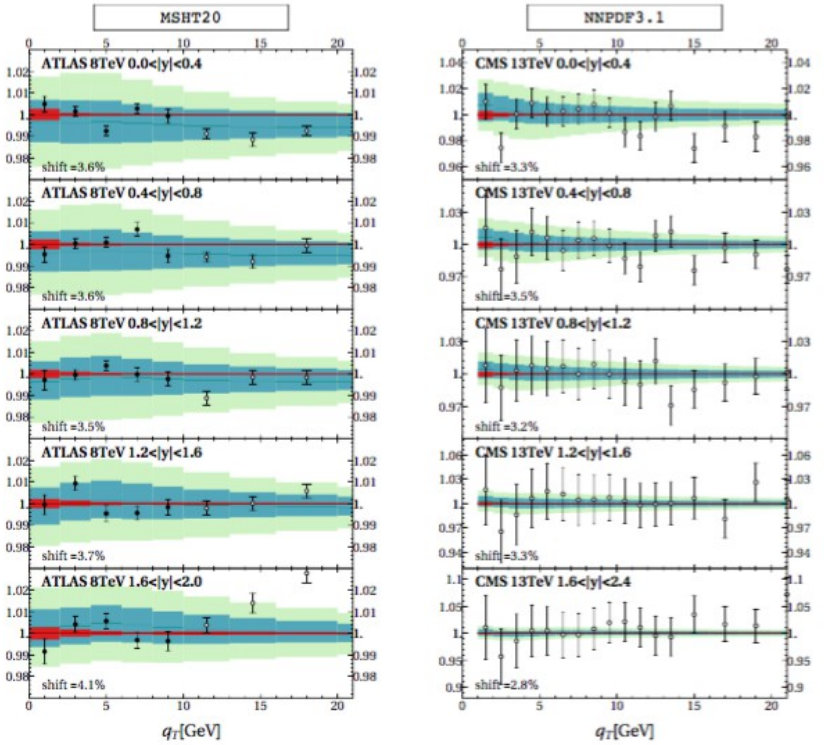

Figure 6: Example of the data description at high energy. Left panel: the ratio $d\sigma_{\text{experiment}}/d\sigma_{\text{theory}}$ for Z-boson production at 8 TeV measured by the ATLAS experiment with MSHT20. Right panel: the ratio $d\sigma_{\text{experiment}}/d\sigma_{\text{theory}}$ for Z-boson production at 13 TeV at the CMS experiment with NNPDF3.1. The red band is the **EXP**-uncertainty. The light-green band is the **PDF**-uncertainty. The blue band is the combined uncertainty. Only the filled bullets are included into the fit.

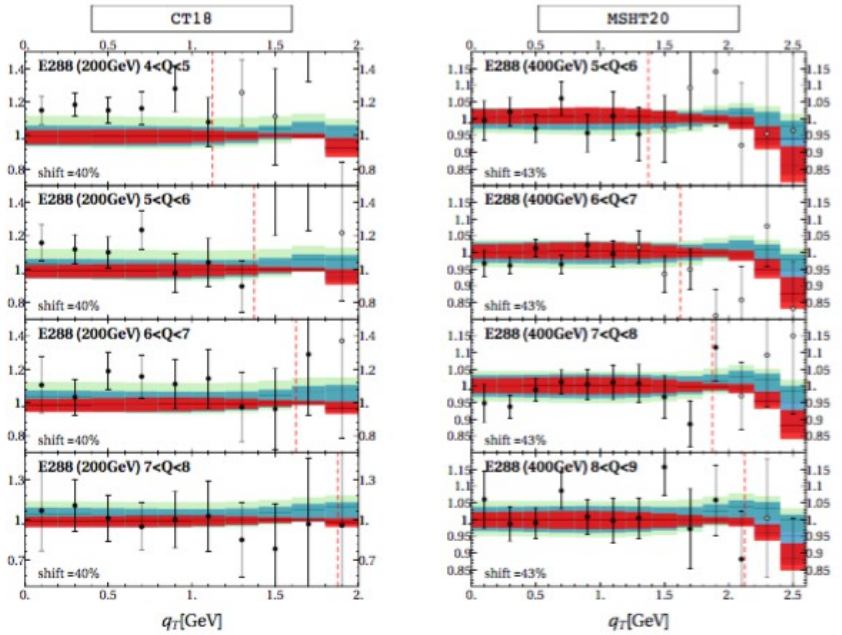

Figure 7: Example of the data description at low energy. Left panel: ratio $d\sigma_{\text{experiment}}/d\sigma_{\text{theory}}$ for the DY process at E288 experiment with 200 GeV beam-energy with CT18. Right panel: ratio $d\sigma_{\text{experiment}}/d\sigma_{\text{theory}}$ for the DY process at E288 experiment with 400GeV beam-energy with MSHT20. Red band is the **EXP**-uncertainty. Light-green band is the **PDF**-uncertainty. The blue band is the combined uncertainty. The filled bullets are included into the fit. The dashed red vertical lines show the expected boundary of the TMD factorization $q_T = 0.25Q$.

Flavour dependence of the TMDs

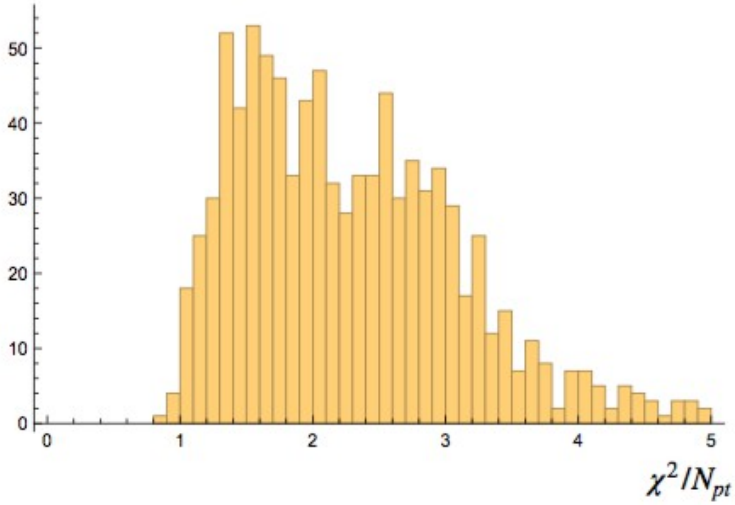

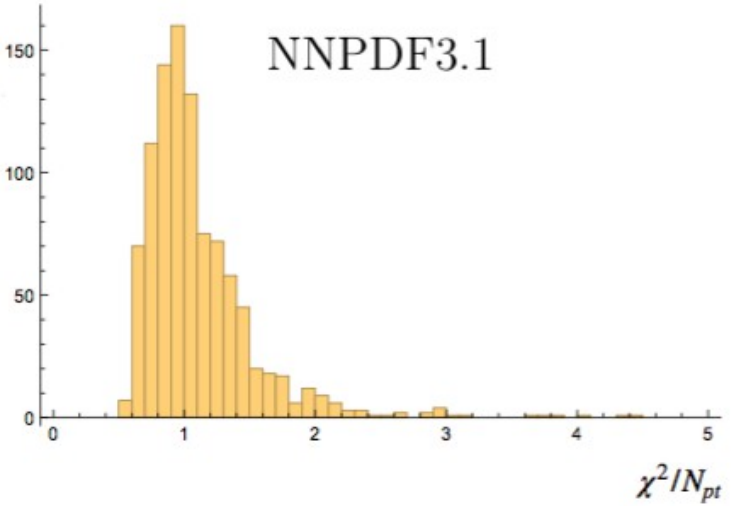

$$f_{NP}(x,b) = \exp\left(-\frac{\lambda_1(1-x)+\lambda_2 x + x(1-x)\lambda_5}{\sqrt{1+\lambda_3 x^{\lambda_4}\mathbf{b^2}}}\mathbf{b^2}\right)$$

$$f^f_{NP}(x,b) = \exp\left(-\frac{\lambda^f_1(1-x)+\lambda^f_2 x}{\sqrt{1+\lambda_0 x^2\mathbf{b^2}}}\mathbf{b^2}\right)$$

$f = u, \bar{u}, d, \bar{d}, sea$

slide by P. Zurita

INCLUSION OF PDF UNCERTAINTY AND FLAVOR DEPENDENCE IN TMD EXTRACTION

Bury et al., arXiv:2201.07114

slide by P. Zurita

- Differences between flavours are clear:
  - **Red** : EXP
  - **Blue** : PDF
  - **Black**: combined

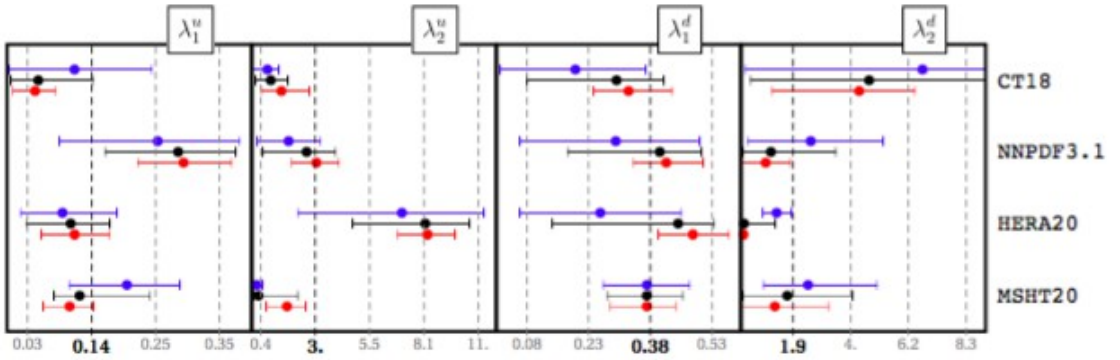

- We obtain realistic uncertainty bands for the TMDPDFs:

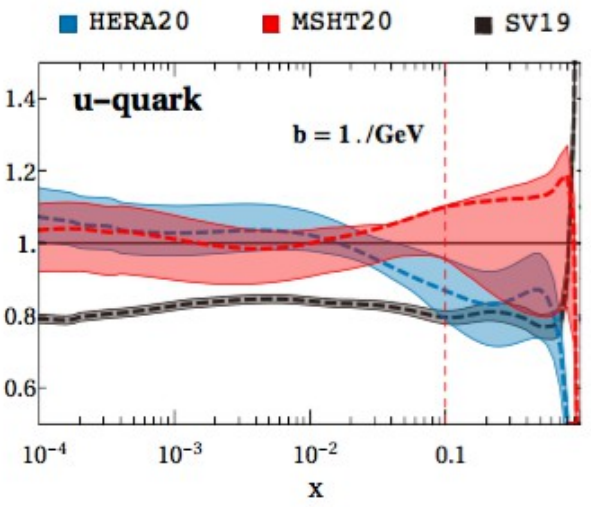

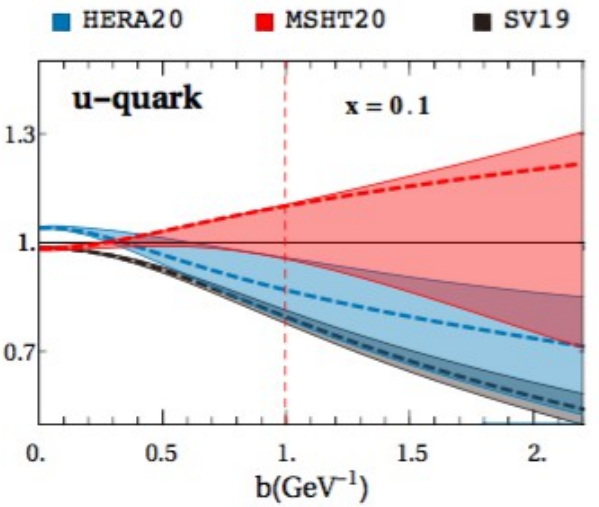

COMMENTS ON RAPIDITY EVOLUTION KERNEL DETERMINATION

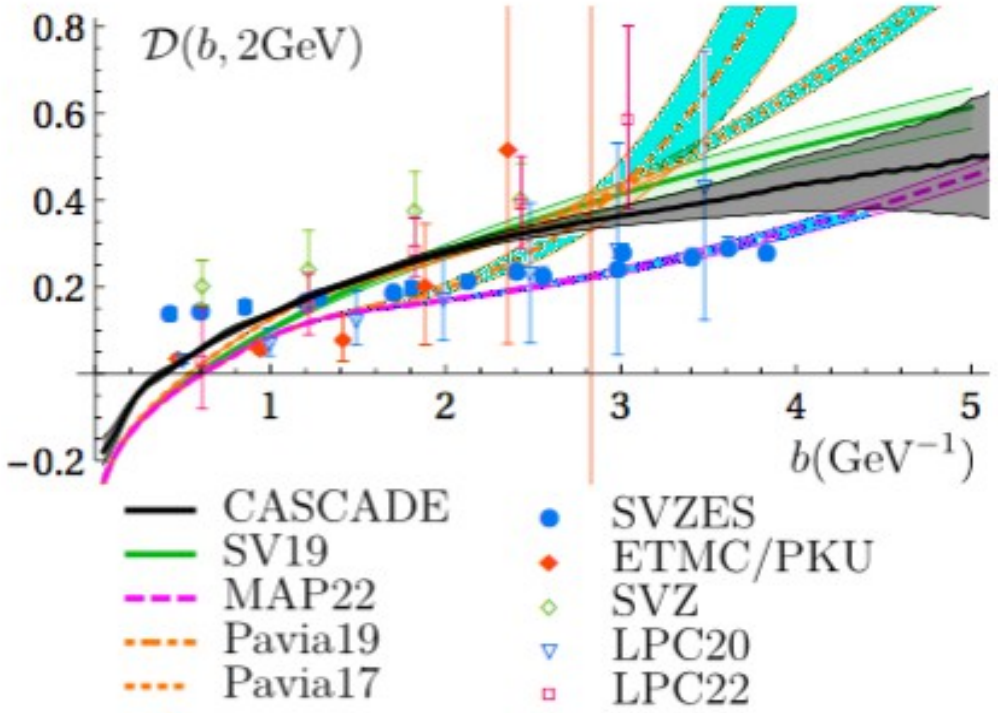

A Bermudez Martinez and A Vladimirov, arXiv:2206.01105

- Impact of PDF, e.g. following the approach just described, yet to be examined on rapidity evolution kernel

- Extractions of the kernel from data fits in this plot assume either quadratic (a la Resbos) or linear behavior at large b.

  Alternative possibility: constant at large b

  [Scimemi, Vladimirov & H, PLB806 (2020) 135478, arXiv:2002.12810]

  (similar in spirit to saturation in s-channel picture of parton evolution)

CONCLUSION

- Toward systematic understanding of nonperturbative TMD contributions
- Key progress from inclusion of PDF uncertainties
- and from flavor dependence in TMD distributions
- Future analyses expected to elucidate correlations in TMD and rapidity evolution kernel determinations

EXTRA SLIDES

Correlation of TMD parameters for different PDF sets

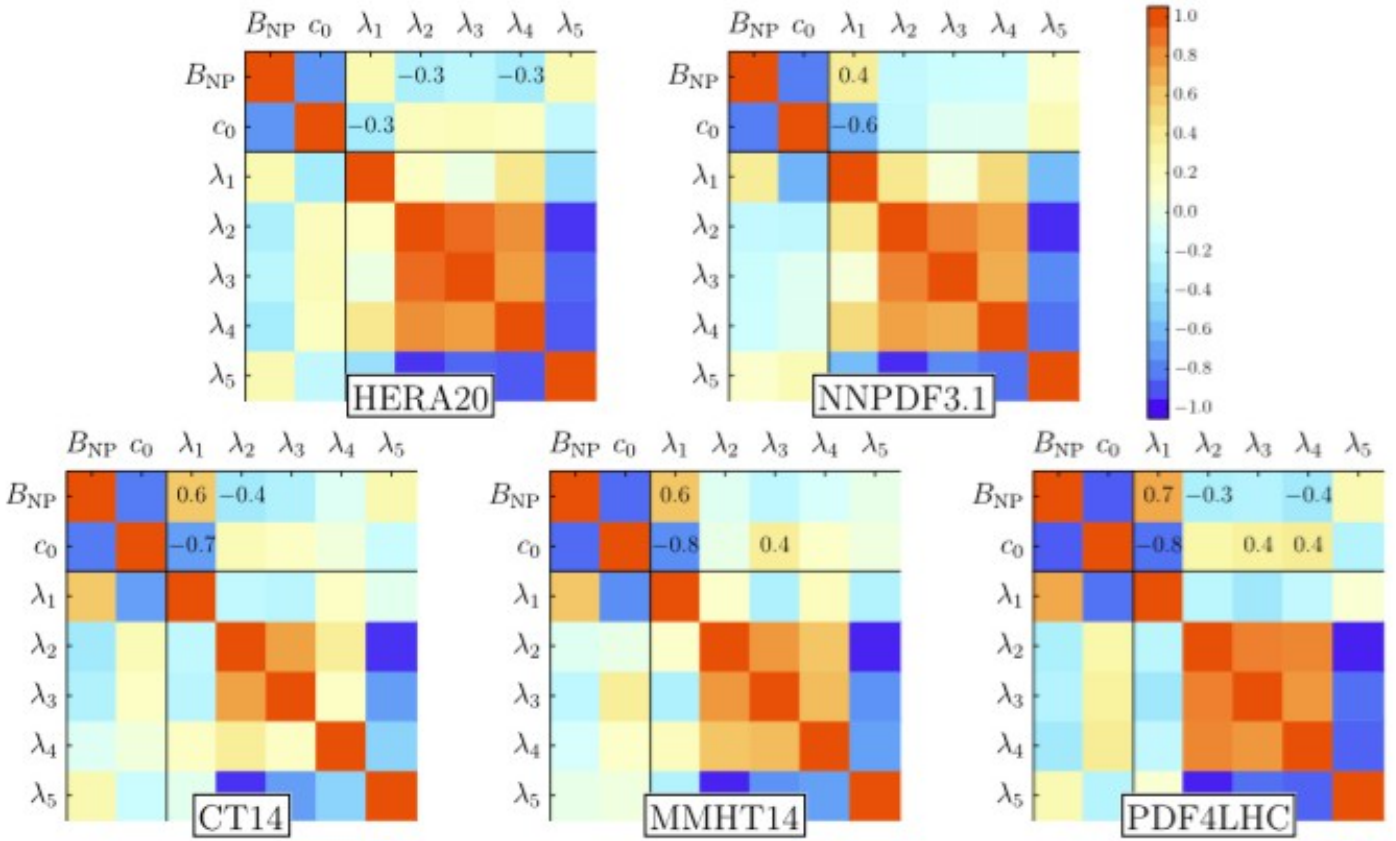

Fig. 3. Correlations of TMD fit parameters. In the axes $1 = B_{NP}$, $2 = c_0$, $(3, 4, 5, 6, 7) = \lambda_{1,2,3,4,5}$. Low correlation is represented by light colors, high correlation by dark colors. (The diagonal entries are trivial.)

- Correlations vary with PDF sets

The cut qT / Q < delta

- We vary the cut delta on the data set

- The delta dependence is mild between 0.1.and 0.25 both for the chi^2 and for the parameter values

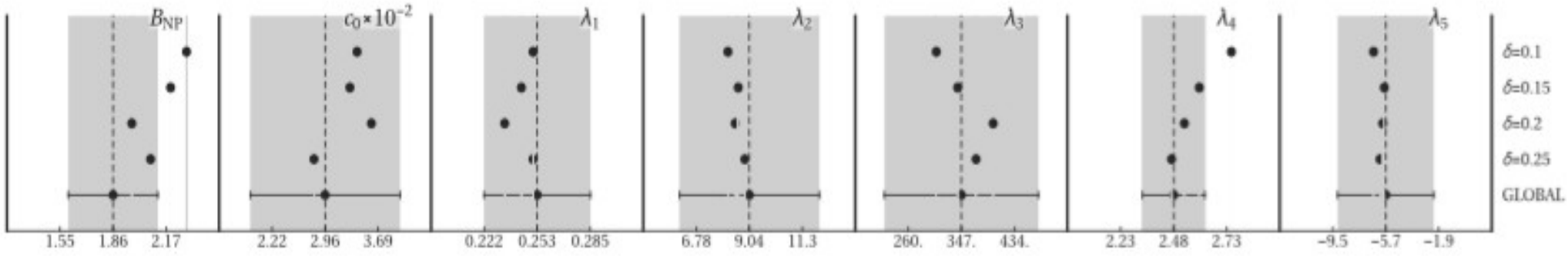

Fig. 2. Dependence of the values of the fitted TMD parameters on the δ cut (NNPDF3.1 PDF set).

- Matching with high qT region is not included yet

The role of precision LHC measurements

2-parameter fits (cases 1, 3, 5): no intrinsic kT
3-parameter fits (cases 2, 4, 6): both nonperturbative Sudakov and intrinsic kT

Case	B_{NP}	g_K	λ_1 ($f_{NP} = \exp -\lambda_1 b^2$)	χ^2/dof	χ^2/dof(norm.)
1	5.5 (max)	0.116 ± 0.002	10^{-3}(fixed)	3.29	3.04
2	2.2 ± 0.4	0.032 ± 0.006	0.29 ± 0.02	1.50	1.28
Case	B_{NP}	c_0	λ_1	χ^2/dof	χ^2/dof(norm.)
3	1. (min)	0.016 ± 0.001	10^{-3}(fixed)	2.21	1.99
4	3.0 ± 1.5	0.04 ± 0.02	0.27 ± 0.04	1.61	1.36
Case	B_{NP}	g_K^*	λ_1	χ^2/dof	χ^2/dof(norm.)
5	1.34 ± 0.01	0.16 ± 0.01	10^{-3}(fixed)	1.70	1.52
6	2.43 ± 0.66	0.05 ± 0.02	0.24 ± 0.04	1.49	1.28

Table 3: Results of 3-parameter and 2-parameter fits. The PDF set used is NNPDF3.1 [63].

- 3-parameter cases similar to global fit results
- Case 6: saturating behavior d D / d ln b = 0

$$R_\sigma = 2\,\frac{d\sigma^{\text{test}} - d\sigma^{TMD}}{d\sigma^{\text{test}} + d\sigma^{TMD}}\,, \qquad (12)$$

- 2-parameter fits lead to higher chi2 values and different fitted parameters for rapidity kernel.
- I.e., intrinsic kT effects may be reabsorbed by changes in D.

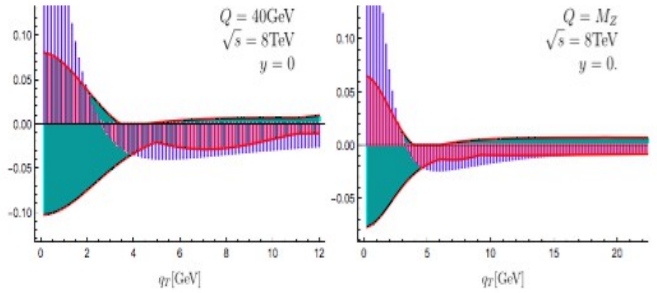

Figure 4: Sensitivity to nonperturbative physics in LHC DY measurements: the transverse momentum dependence of the ratio in Eq. (12), for central rapidity and different values of the lepton-pair invariant mass. The solid band is obtained from perturbative scale variation.

Given the reduction of perturbative uncertainties due to high logarithmic accuracy, residual uncertainty from nonperturbative TMD effects is non-negligible at low qT and increasing with decreasing masses.

Nonperturbative contributions I: rapidity evolution kernel

- Write D using b* prescription as

$$\mathcal{D}^f(\mu, \boldsymbol{b}) = \mathcal{D}^f_{\rm res}(\mu, b^*(\boldsymbol{b})) + g(\boldsymbol{b}), \qquad \text{where} \qquad b^*(\boldsymbol{b}) = |\boldsymbol{b}| \sqrt{\frac{B_{\rm NP}^2}{\boldsymbol{b}^2 + B_{\rm NP}^2}}$$

- Nonperturbative component of rapidity evolution kernel modeled and fitted to data:

$$g(\boldsymbol{b}) = g_K \boldsymbol{b}^2,$$

quadratic behavior
(traditionally used in TMD fits since Resbos)

$$g(\boldsymbol{b}) = c_0 |\boldsymbol{b}| b^*(\boldsymbol{b}),$$

linear rise at large b

$$g(\boldsymbol{b}) = g_K^* \boldsymbol{b}^{*2},$$

quadratic at small b, constant at large b
(similar spirit to parton saturation in s-channel picture *[Soper & H, PRD 75 (2007) 074020]*)
d D / d ln b = 0 for large b

- Zeta prescription scale setting *[A. Vladimirov, arXiv:1907.10356]*

$$\zeta_{\rm NP}(\mu, b) = \zeta_{\rm pert}(\mu, b) e^{-b^2/B_{\rm NP}^2} + \zeta_{\rm exact}(\mu, b)\left(1 - e^{-b^2/B_{\rm NP}^2}\right).$$

RAPIDITY EVOLUTION KERNEL

- Red curves: quadratic D; yellow curves: saturating D; blue curves: linear D.
- For each color, difference between solid and dashed curves measures correlations between Sudakov and intrinsic kT effects.

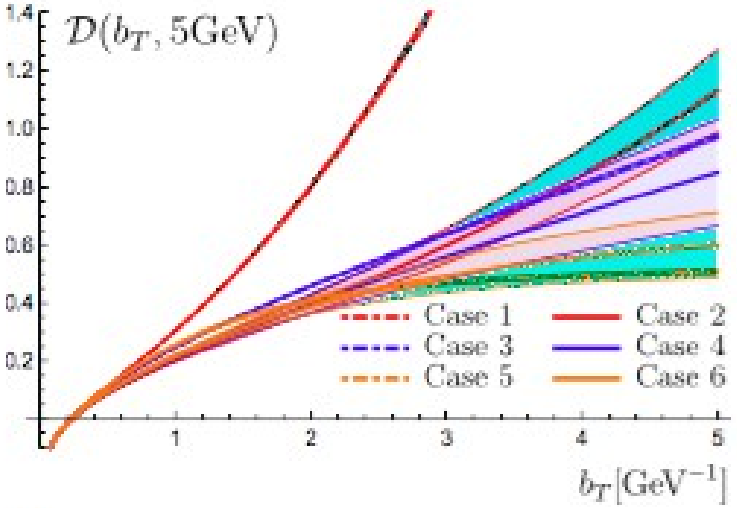

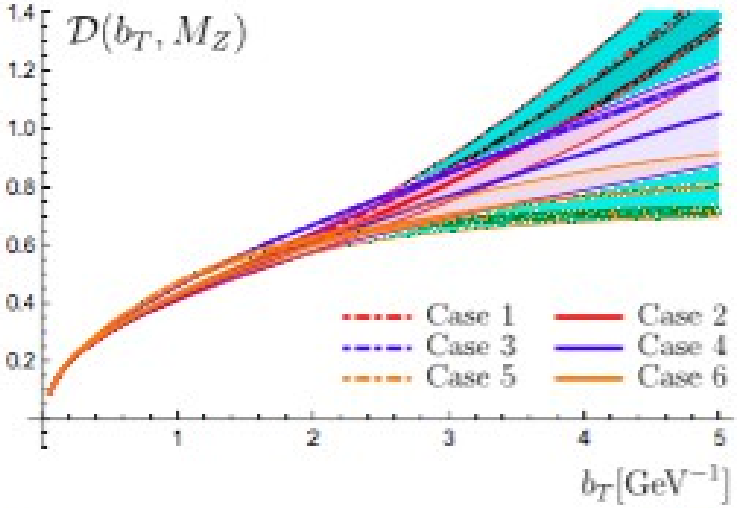

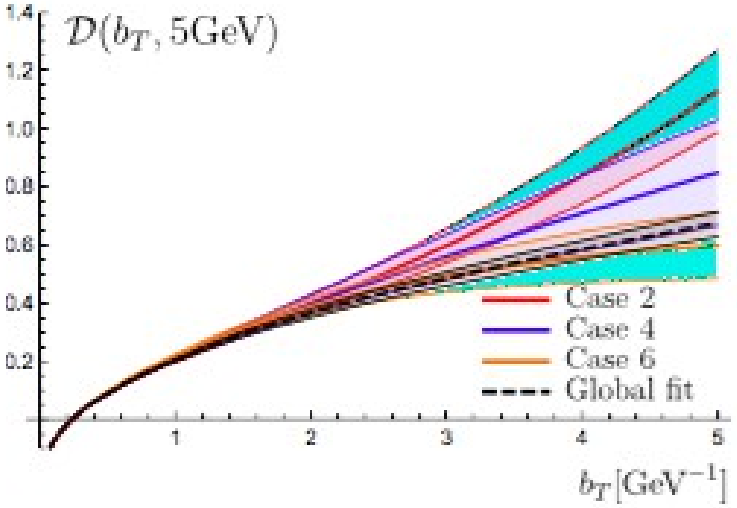

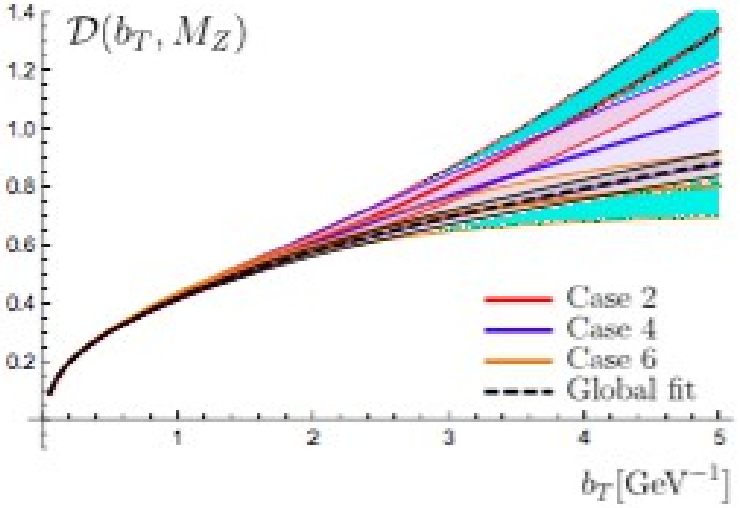

Quadratic model implies more pronounced dependence on intrinsic kT than the others (showing up especially for low masses)

RAPIDITY EVOLUTION KERNEL

- Limited sensitivity of current LHC measurements to long-distance region results into sizeable uncertainty bands at large b
- Higher sensitivity from low-qT measurements with fine binning in qT at low masses

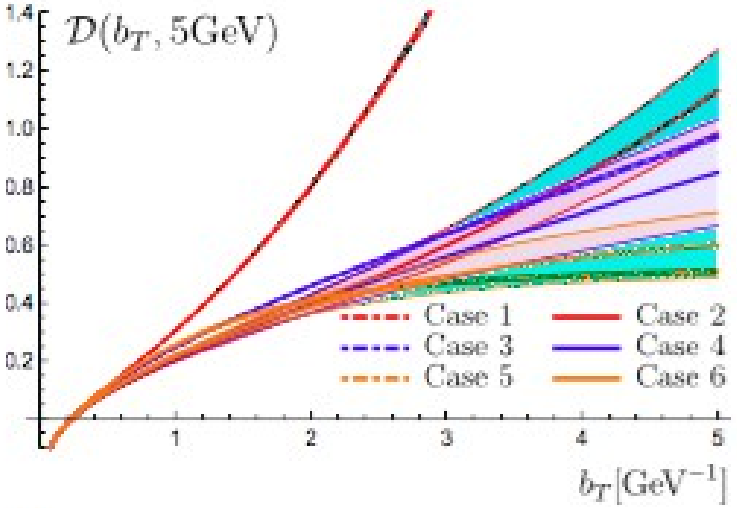

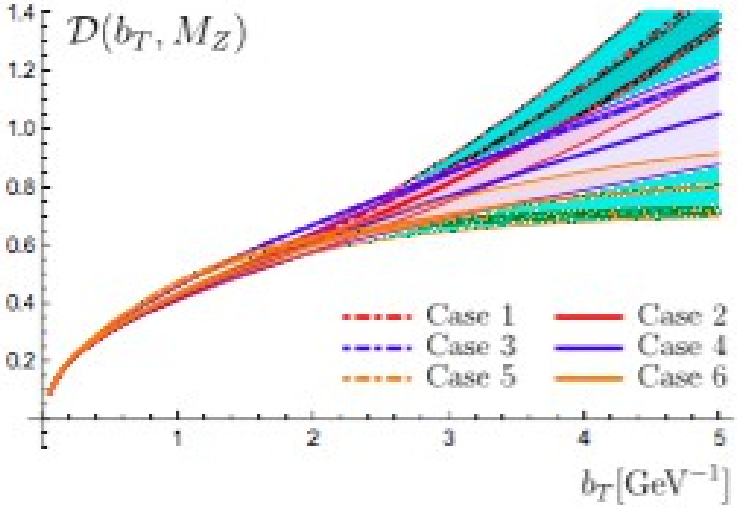

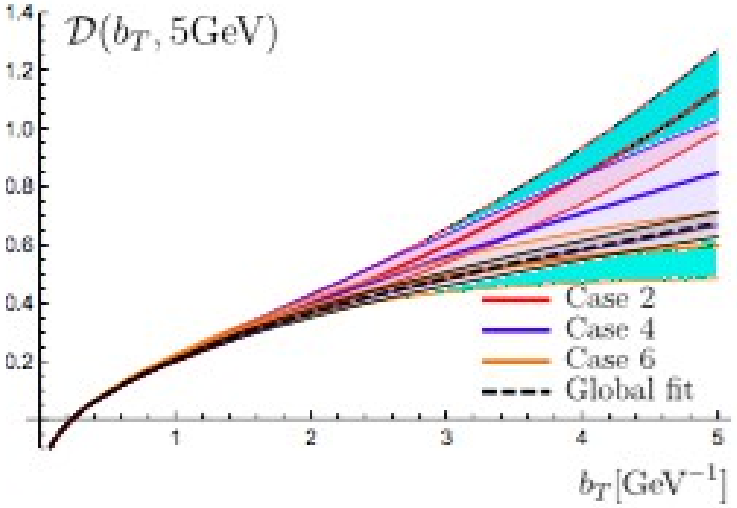

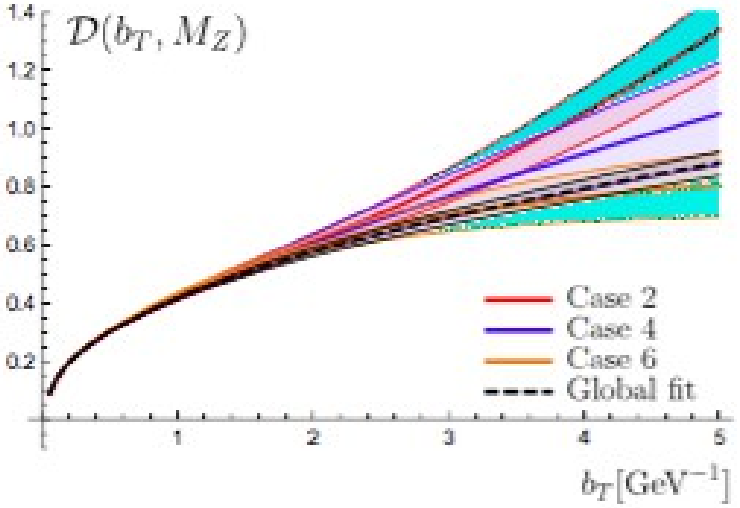

- Global fit result in lower panels illustrates role of low-energy data: performed with linear model – but lower than blue curve and closer to yellow (saturating) curve

Remarks

- Used low-qT TMD factorization to investigate sensitivity of LHC and low-energy DY measurements to nonperturbative f and D, and correlations with collinear PDFs.
- Although strongest nonperturbative sensitivity is from low energy, neglecting any intrinsic kT at the LHC worsens quality of fits and causes potential bias in determination of rapidity evolution kernel
- Residual uncertainty from nonperturbative TMD effects non-negligible in lowest qT bins (increasing with decreasing masses)
- Results on large-b behavior of rapidity evolution kernel complementary to lattice studies – e.g. linear vs. saturating behavior
- Matching with high qT region yet to be included

Inclusion of PDF uncertainty in TMD extraction

- EXP: 100 replicas of the data.
- PDF: 1000 replicas of the PDFs.

- For each case we obtain a set of parameters which are then combined in a weighted average to give the final result.

- More importantly:

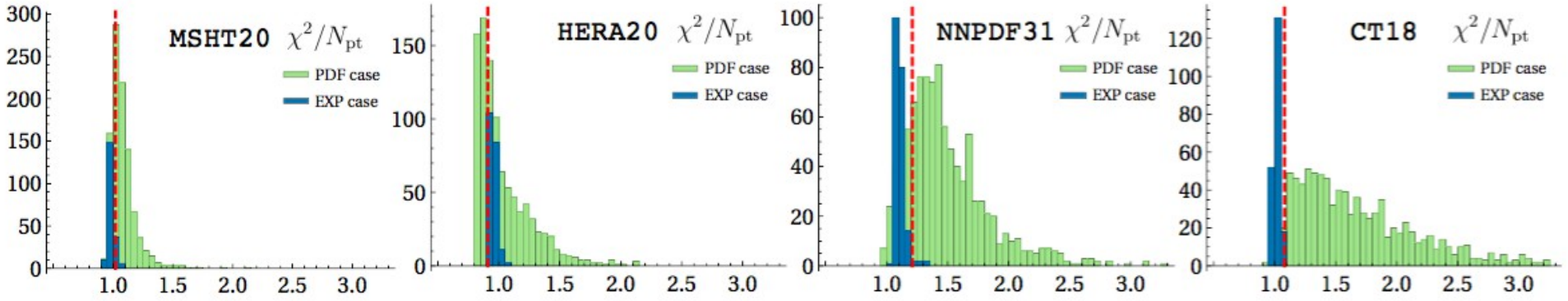

Extracted TMD parameters

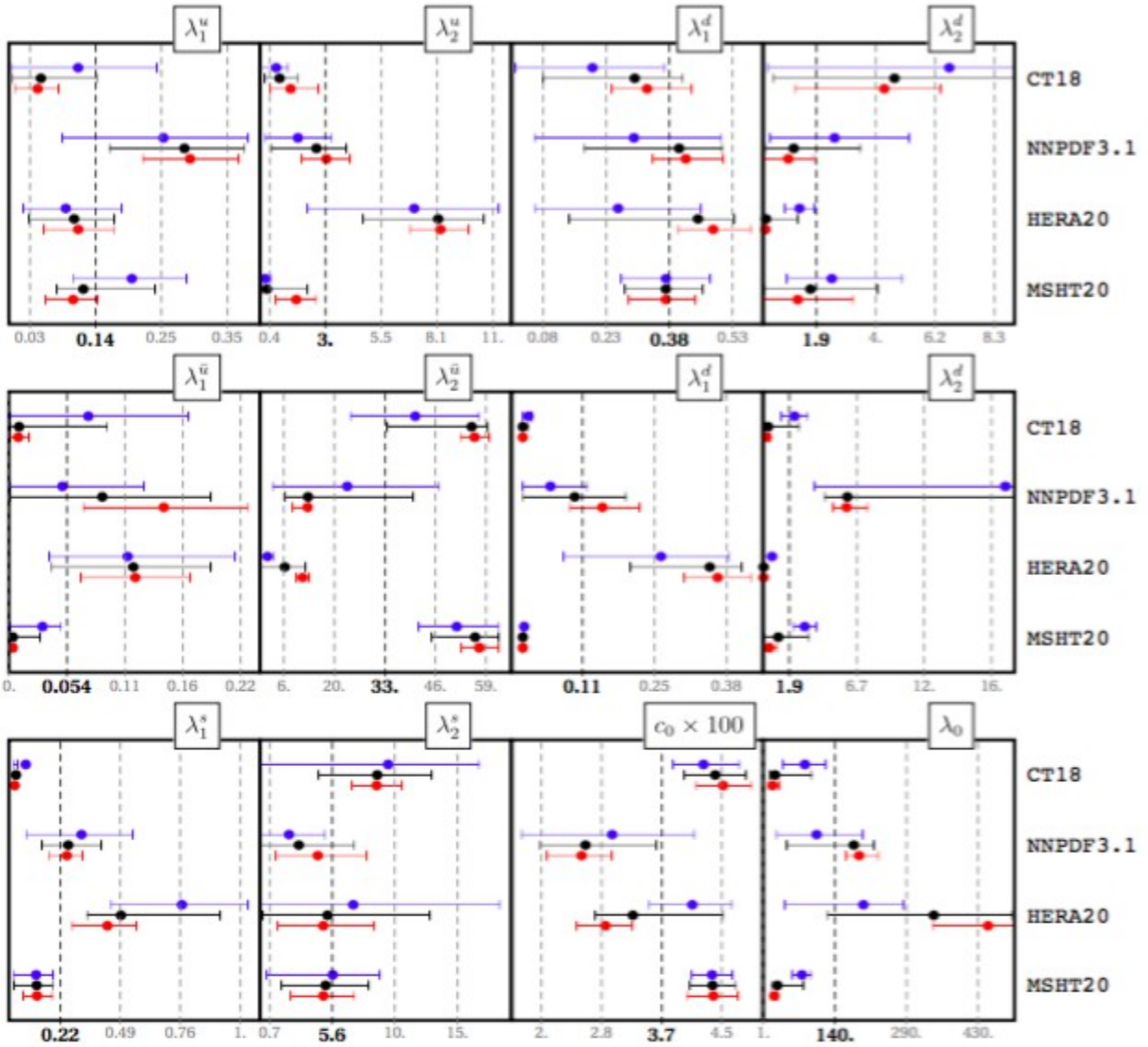

Figure 8: Comparison of the parameter values. Black is the final result. Blue is the value from the fit of the **PDF** case. Red is the value from the fit of the **EXP** case.

TMD uncertainties

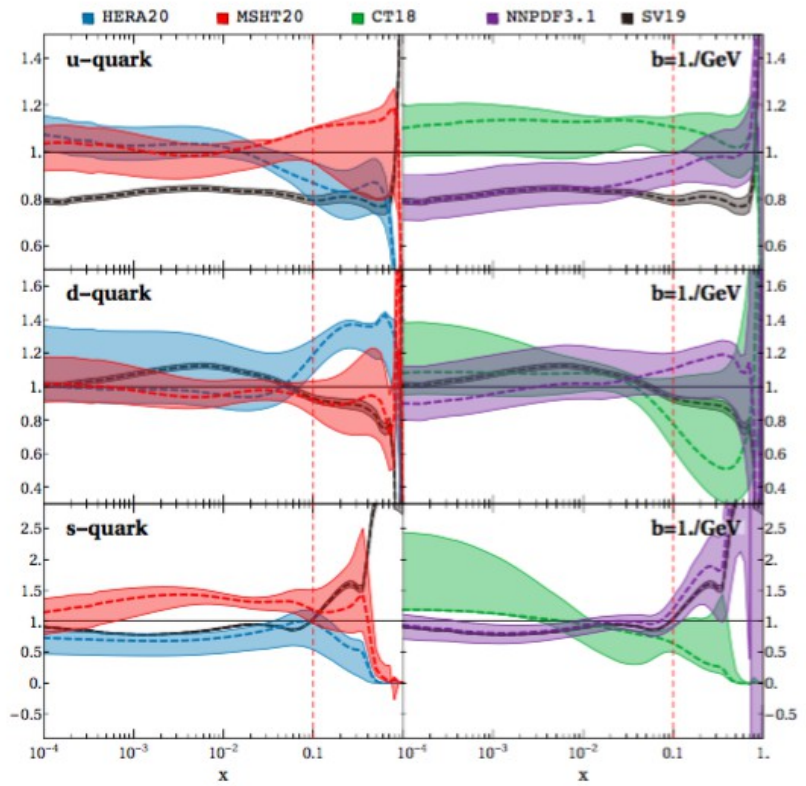

Figure 10: Comparison of uncertainty band for unpolarized TMDPDFs extracted with different PDFs. Here, the slice of optimal TMDPDF at $b = 1\text{GeV}^{-1}$ is shown as the function of x. For convenience of presentation the plot is weighted with the central TMDPDF value averaged between different PDF cases. The red line indicates the position of slice demonstrated in fig.11.

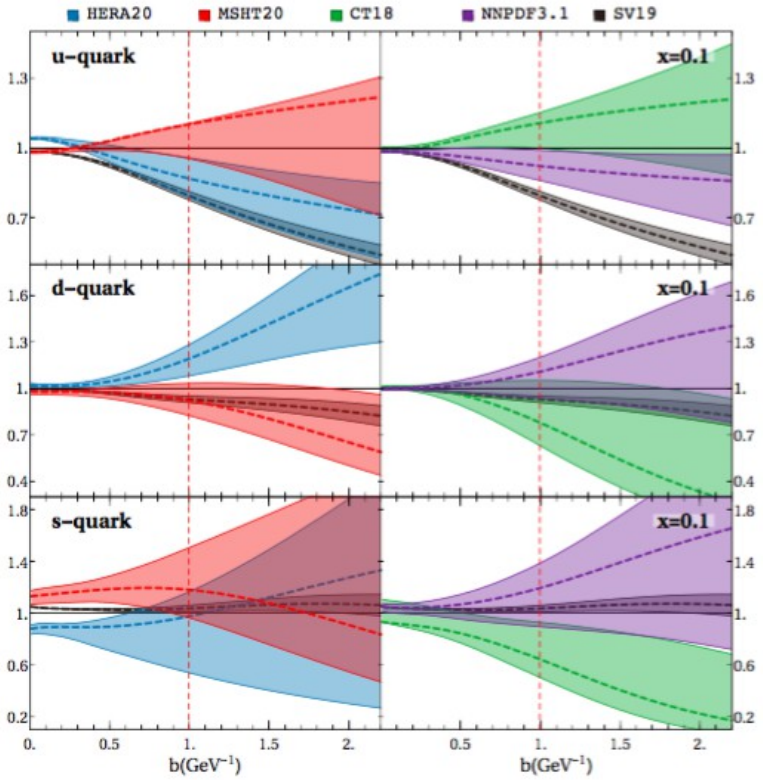

Figure 11: Comparison of the uncertainty band for unpolarized TMDPDFs extracted with different PDFs. Here, the slice of optimal TMDPDF at $x = 0.1$ is shown as a function of b. For convenience of presentation the plot is weighted with the central TMDPDF value averaged between different PDF cases. The red line indicates the position of slice demonstrated in fig. 10.